# Retinoic acid and cAMP inhibit rat hepatocellular carcinoma cell proliferation and enhance cell differentiation

M. Ionta, M.C. Rosa, R.B. Almeida, V.M. Freitas, P. Rezende-Teixeira and G.M. Machado-Santelli

# Retinoic acid and cAMP inhibit rat hepatocellular carcinoma cell proliferation and enhance cell differentiation

M. Ionta[1,2], M.C. Rosa[2], R.B. Almeida[2], V.M. Freitas[2], P. Rezende-Teixeira[2] and G.M. Machado-Santelli[2]

[1]Instituto de Ciências Biomédicas, Universidade Federal de Alfenas, Alfenas, MG, Brasil
[2]Departamento de Biologia Celular e do Desenvolvimento, Instituto de Ciências Biomédicas, Universidade de São Paulo, São Paulo, SP, Brasil

## Abstract

Hepatocellular carcinoma (HCC) is the third highest cause of cancer death worldwide. In general, the disease is diagnosed at an advanced stage when potentially curative therapies are no longer feasible. For this reason, it is very important to develop new therapeutic approaches. Retinoic acid (RA) is a natural derivative of vitamin A that regulates important biological processes including cell proliferation and differentiation. *In vitro* studies have shown that RA is effective in inhibiting growth of HCC cells; however, responsiveness to treatment varies among different HCC cell lines. The objective of the present study was to determine if the combined use of RA (0.1 µM) and cAMP (1 mM), an important second messenger, improves the responsiveness of HCC cells to RA treatment. We evaluated the proliferative behavior of an HCC cell line (HTC) and the expression profile of genes related to cancer signaling pathway (ERK and GSK-3β) and liver differentiation [E-cadherin, connexin 26 (Cx26), and connexin 32 (Cx32)]. RA and cAMP were effective in inhibiting the proliferation of HTC cells independently of combined use. However, when a mixture of RA and cAMP was used, the signals concerning the degree of cell differentiation were increased. As demonstrated by Western blot, the treatment increased E-cadherin, Cx26, Cx32 and Ser9-GSK-3β (inactive form) expression while the expression of Cx43, Tyr216-GSK-3β (active form) and phosphorylated ERK decreased. Furthermore, telomerase activity was inhibited along treatment. Taken together, the results showed that the combined use of RA and cAMP is more effective in inducing differentiation of HTC cells.

Key words: Cell adhesion; cAMP; Differentiation; Proliferation; Hepatocarcinoma; Retinoic acid

## Introduction

Hepatocellular carcinoma (HCC) is a major healthcare problem worldwide representing the fifth leading cause of cancer mortality and the third most common cause of cancer-related deaths (1). The development of HCC is frequently associated with chronic viral infection (hepatitis B virus or hepatitis C virus); however, frequent exposure to toxic agents (alcohol or aflatoxin) can contribute to the development of HCC (2).

In general, HCC is diagnosed in advanced stages when potentially curative therapies are not feasible. Only a minority of HCC are detected at an early enough stage for potentially curative therapies, such as surgical resection, liver transplantation or local ablation therapy. Thus, the development of alternative therapeutic approaches to HCC remains one of the most challenging areas of cancer research.

Retinoic acid (RA) is an active metabolite of vitamin A that regulates important biological processes such as cell proliferation, cell differentiation and cell death (3). It has been reported that RA inhibits the proliferation of malignant tumor cells; however, its negative effect on cell growth is dose-dependent and cell-specific (4).

It is well known that RA not only induces growth inhibition of leukemia cells, but also stimulates their maturation. RA has been used as a chemotherapeutic agent in patients with acute promyelocytic leukemia (APL) since 1985 (5). Since then, the activity of RA on cell proliferation has been investigated in tumor cells derived from solid tumors, in-

cluding HCC (6-8).

Jung et al. (9) carried out an interesting study working with 4 different HCC cell lines (HepG2, SNU354, Hep3B, and SNU449). They verified that RA inhibited cell growth in only two cell lines (HepG2 and SNU354). Curiously, the proliferative behavior of Hep3B and SNU449 cells was stimulated by treatment with RA. These results clearly show that HCC present distinct responsiveness to RA depending on their characteristics.

The combined use of two or more drugs can be advantageous in chemotherapy. Drug dosage would be lower, thus decreasing toxicity. Furthermore, a combination of drugs may improve treatment responsiveness through synergistic effects.

It was reported that RA induces the maturation of APL cells when used at concentrations close to physiological levels (1.0 to 10 nM) due to a sustained increase of the endogenous level of cAMP (10). cAMP is a second messenger that can act as a pro- or anti-mitotic agent depending of both cell type and the physiological state of the cell. The antiproliferative activity of cAMP on HCC cells has been demonstrated in some studies. Lee et al. (11) showed G1 synchronization of HepG2 cells due to down-regulation of cyclin A expression. In BEL-7402 cells, cAMP induced Akt inactivation with consequent inhibition of proliferation (12). Using a rat model of HCC, Kovac et al. (13) demonstrated that cAMP can inhibit cell mitogenesis.

The objective of the present study was to investigate the effects of the combined use of RA and cAMP on the proliferative behavior and phenotype of an HTC cell line derived from rat HCC. Our results showed that both RA and cAMP inhibit the proliferation of HTC cells. Moreover, the period of inhibition was greater in cells that received the mixture than in those treated with either RA or cAMP alone. Another advantage of the RA and cAMP combination is the degree of differentiation achieved. HTC cells treated with the drug mixture presented a more differentiated phenotype. Thus, the combined use of RA and cAMP extended growth inhibition and increased the degree of differentiation of HCC cells.

## Material and Methods

### Cell culture conditions

The rat HCC cell line (HTC) used in this study was acquired from the Cell Bank of Rio de Janeiro (14). The cultures were maintained in Dulbecco's modified Eagle's minimum essential medium (DMEM; Sigma, USA) supplemented with 5% fetal bovine serum (FBS; Cultilab, Brazil). Cells were grown at 37°C in a humidified incubator containing 5% $CO_2$ and subcultured every 2 or 3 days.

### Drugs and treatment schedule

Stock solutions of 1 mM RA (Sigma) and 100 mM cAMP (Sigma) were prepared and diluted in DMEM (supplemented with 5% FBS) to a final concentration of 0.1 μM RA and 1 mM cAMP. Drugs were used alone or in combination and were added on the 3rd day after plating. The treatment schedule was standardized using BRL3A, a non-tumoral cell line that presents great responsiveness to the drugs used (Figure 1). HTC cells were treated for 2 days (T0). After this period, the medium was replaced with drug-free medium and the cultures were tested for recovery at 24 (T24) and 48 h (T48).

### Bromodeoxyuridine (BrdU) incorporation

Cells were cultured on coverslips in 35-mm dishes at 5 x $10^3$ cells/plate. On the testing days, 100 μM BrdU (Sigma)



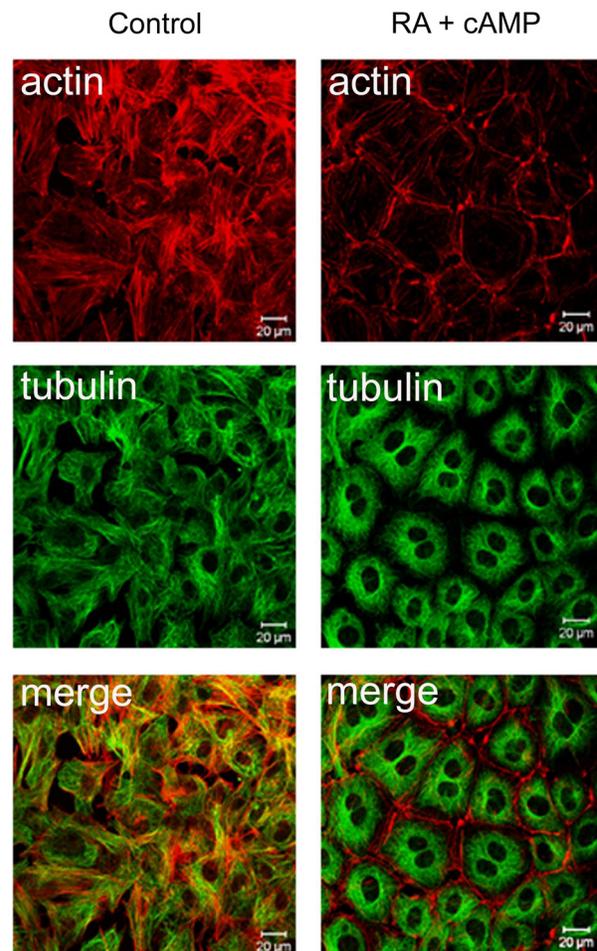**Figure 1.** Laser scanning confocal microscopy images of BRL3A cells showing the actin filament distribution pattern at T48. The morphology of cells is demonstrated by F-actin staining (red) and anti-tubulin immunoreaction (green). Retinoic acid (RA) and cAMP induced cytoskeleton reorganization and a change in cell shape to polyhedric. Note the presence of binucleated cells in the images that indicate microtubule networks.

was added to the medium for 1 h. The cells were fixed in ethanol:acetic acid (3:1) for 30 min and the immunofluorescence assay was performed as described by Prado et al. (15). Mouse anti-BrdU antibody (Sigma) was incubated (1 h) in a wet chamber at room temperature. After washes in Dulbecco's phosphate-buffered saline (PBSA), the secondary antibody (anti-mouse IgG-FITC, Sigma) was incubated for 2 h. The nuclei were stained with 10 µg/mL propidium iodide and the coverslips were mounted on histological slides with Vecta-Shield (Vector Laboratories, USA). The analyses were performed using fluorescence microscopy (Zeiss, Germany). One thousand cells were counted in each sample. Three independent experiments were performed and the data are reported as means ± SD.

## Mitotic index

Cells were cultured on coverslips in 35-mm dishes at $5 \times 10^3$ cells/plate. On the indicated days cells were fixed in ethanol:acetic acid (3:1) for 30 min at room temperature and stained by the Feulgen reaction as described by Machado-Santelli et al. (16). Metaphase frequency was determined in one thousand cells counted in each sample. Data are reported as means ± SD for three independent experiments.

## Cytoskeleton elements: microtubules and F-actin

Cells were cultured on coverslips in 35-mm dishes at $5 \times 10^3$ cells/plate. Cells were fixed with 3.7% formaldehyde for 30 min, and the cell membrane was permeabilized with 0.5% Triton X-100 for 10 min. Cells were incubated overnight with mouse monoclonal primary antibodies (anti-α and anti-β tubulin diluted in PBSA at 1:200 and 1:100, respectively) in a wet chamber at 4°C. A secondary antibody (anti-mouse IgG-FITC, Sigma) was added for 2 h and the microfilaments were stained with TRITC-phalloidin for 20 min. Coverslips were mounted on histological slides with Vecta-Shield (Vector Laboratories). The analyses were performed using a confocal laser scanning microscope (LSM 510, Zeiss). The lasers used were argon (488 nm) and helium-neon (543 nm) connected to an inverted fluorescence microscope (Axiovert 100M, Zeiss). Binucleated cells were quantified in fluorescent preparations by analyzing 1000 cells per slide. Data are reported as means ± SD for three independent experiments.

## PCR-ELISA telomerase assay

Quantitative determination of telomerase activity was performed according to the Telomeric Repeat Amplification Protocol using the TeloTAGGG Telomerase PCR ELISA[PLUS] kit (Roche Diagnostic GmbH, Germany). Briefly 2 x 10^5 cells were lysed using 2 mL lysis buffer and centrifuged at 4°C for 30 min at 13,000 rpm. The supernatants of different samples were divided into two aliquots before performing the assay: one was used as negative control after heat inactivation of telomerase at 80°C for 10 min and the other was used to evaluate the telomerase-mediated addition of the telomeric sequence. The products obtained were amplified by PCR. To exclude false-negative results due to Taq DNA-polymerase inhibitors eventually present in the lysates, a 216-bp long internal standard, present in the reaction mixture, was simultaneously amplified. The results are reported as relative telomerase activity (RTA), which was calculated according to the following formula: RTA = [(Abs sample - Abs RNAase-treated sample) / Abs internal standard of the sample] / [(Abs control template - Abs lysis buffer) / Abs internal standard of the control template] x 100, where Abs = absorbance.

## Immunoblotting

Cells were cultured in 75-cm^2 flasks, washed with cold PBSA and scraped into radioimmunoprecipitation assay buffer (150 mM NaCl, 1.0% Nonidet P-40, 0.5% deoxycholate, 0.1% SDS, and 50 mM Tris, pH 8.0) with both protease and phosphatase inhibitors (Sigma). Lysates were centrifuged at 10,000 $g$ for 10 min at 4°C. The supernatants were recovered, protein was quantified using a bicinchoninic acid kit (Pierce Biotechnology Inc., USA) and resuspended in Laemmli sample buffer containing 62.5 mM Tris-HCl, pH 6.8, 2% SDS, 10% glycerol, 5% mercaptoethanol, and 0.001% bromophenol blue. A 30-µg protein aliquot was separated by SDS-PAGE (10%) and transferred (100 V, 250 mA for 2 h) to a polyvinylidene fluoride membrane (Amersham Bioscience, USA). The blocking solution (Tris-buffered saline and 0.05% Tween 20 = TTBS plus 5% skim milk) was added at 4°C for 1 h. The membrane was probed with different antibodies [anti-connexin 43 (Cx43) mouse monoclonal antibody, Sigma (1:500); anti-Cx32 mouse monoclonal antibody, Sigma (1:300); rabbit polyclonal anti-Cx26 antibody, Sigma (1:500); anti-vimentin, Chemicon (1:300, USA); anti-pERK (phosphorylated extracellular signal-regulated kinase), anti-ERK, anti-Ser9-pGSK-3β (phosphorylated glycogen synthase kinase 3 beta), anti-Tyr216-pGSK-3β and anti-E-cadherin antibodies, Santa Cruz (1:500, USA)]. All blots were incubated with the antibodies overnight. After washing with TTBS, anti-mouse or anti-rabbit peroxidase-conjugated antibodies were added for 2 h at room temperature. The immunoreactive bands were visualized with the ECL Western blotting detection kit (Amersham Pharmacia) according to manufacturer instructions. Anti-α-tubulin antibody was used as control to check loading conditions.

## Cell adhesion assay

Adhesion assay was performed on 96-well round-bottomed plates. Wells were coated with 100 µL laminin-111 (1 µg/well) overnight at 4°C. Wells were blocked with 3% BSA for 30 min at 37°C and rinsed in 0.1% BSA. The cells were maintained in a humidified incubator containing 5% $CO_2$ at 37°C for 20 min. After attachment, the cells were fixed/stained for 10 min with 0.2% (w/v) crystal violet in 20% (v/v) methanol. After three washes with $H_2O$, cells

were dissolved in 10% (w/v) SDS, and the absorbance at 600 nm was measured. The experiment was performed in triplicate and data are reported as means ± SD.

### Statistical analysis

The quantitative data are reported as means ± SD. ANOVA was performed and the experiments were carried out in triplicate. We also applied the Bonferroni multiple comparisons test. The Graphpad Prism software (GraphPad Software, Inc., USA) was used.

## Results

### Standardization of the treatment schedule

To determine the treatment schedule, we used the BRL3A cell line, a lineage established from rat normal liver. The assays performed with BRL3A cells showed that RA alone was able to induce cell differentiation; however, the cell population with a differentiated phenotype was more expressive when RA was associated with cAMP. We observed drastic changes in morphology of BRL3A cells as well as a significant increase in the frequency of binucleated cells, an important indicator of a differentiated phenotype in hepatic cells. Thus, we used the same treatment schedule for HTC cells, e.g., 48 h of treatment (RA and cAMP used in combination or not) followed by 24- and 48-h recovery in fresh medium.

### Cell proliferation

HTC cells treated with RA and/or cAMP for 48 h exhibited a decrease in cell proliferation, as demonstrated by BrdU incorporation and mitotic index (Figure 2). Immediately after the treatments (T0) the mitotic indexes were lower than control independently of the type of treatment (3.7% for the control, 2.5% for RA, 1.84% for cAMP, and 1.78% for RA plus cAMP). After 24 h of recovery (T24), the mitotic index reached 5.6% in controls as opposed to 0.6, 2.63, and 2.16% for cells treated with RA, cAMP and RA plus cAMP, respectively. At T48, the cells seemed to recover their proliferation capacity, and the mitotic indexes of the treated cells were similar to control. The percentage of cells in the S-phase at T0 was higher in the control culture (33.76%) compared to treated cultures (24.1% in RA, 20% in cAMP, and 20% in RA plus cAMP). After a 24-h recovery, BrdU indexes were similar for cAMP-treated and control cells while the S-phase indexes for RA or cAMP plus RA cells remained lower. After a 48-h recovery, the only difference was observed in the RA-treated group, with no differences among the other three groups.

### Cell differentiation

*Morphology and adhesion capacity*. HTC is a pleomorphic cell line, which contains cells with different morphological features. This aspect is probably related to differences in cell-to-substrate adhesion levels, as indicated by the

observation of flattened cells that adhere to the substrate and rounded cells that grow only partially adhered to the substrate (Figure 3A and B). Figure 3 shows different optical sections obtained by confocal LSM of cytological preparations stained with TRITC-phalloidin at T48. In the treated cultures, we only observed cells growing tightly adhered to the substrate (Figure 3C-H). These cells exhibited actin stress fibers that were widely distributed in the cytoplasm (Figure 3C, E and G). The pattern of microfilament distribution in the treated cells was very similar to that observed in BRL3A cells, a non-tumoral liver cell line (data not shown). Another important aspect of treated cultures was the cellular arrangement. The cells treated with RA and RA plus cAMP (Figure 3C,D and G,H) were arranged in a rope-like manner. Interestingly, cAMP treatment increased the frequency of binucleated cells (Figure 3E and F). At T48 (the time point of immunofluorescent confocal images), 0.3% of cells were binucleated in control cultures compared to 0.5, 1.1, and 1.13% in cultures treated with RA, cAMP and RA plus cAMP, respectively.
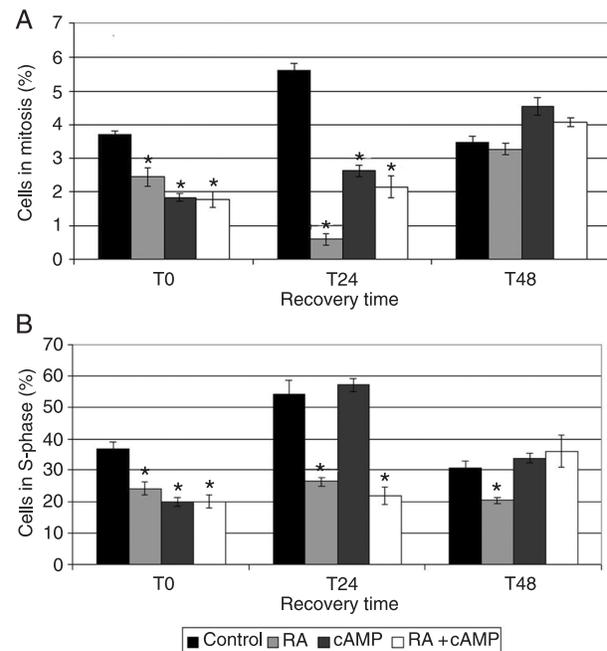


**Figure 2.** Cell proliferation behavior of hepatocellular carcinoma (HCC) cells as indicated by mitotic index (*A*) and S-phase cell population (*B*). Data are reported as % total cells. Mitotic indexes were significantly lower in cultures treated with retinoic acid (RA), cAMP and RA plus cAMP when compared to the control culture at T0 and T24. S-phase cell population frequencies were lower in all treated cultures compared to control at T0. At T24, cultures treated with RA alone and RA plus cAMP presented lower S-phase populations compared to control. At T48, only cultures treated with RA presented lower S-phase population than control. *P < 0.05, compared to control (Bonferroni test).

The pattern of microtubule distribution changed according to treatment. This was clearly shown in the projections of Z-stack optical slices from the confocal LSM in a single plane image (Figure 4). The microtubules were seen more clearly in treated cells than in control cells. Both RA and cAMP changed the organization pattern of microtubules.

Cell adhesion to the substrate was improved by the treatments. We observed that both RA and cAMP increased the adhesion capacity of treated cells to the laminin substrate at T0 and T24 (Figure 5).

## Connexin, E-cadherin and vinculin expression

HTC cells preferentially express Cx43, compared to low levels or absence of Cx32 or Cx26 expression. This pattern of connexin expression did not change at T0, but changes in connexin expression profiles were observed at T24 and T48. At T24, we detected expression of Cx32
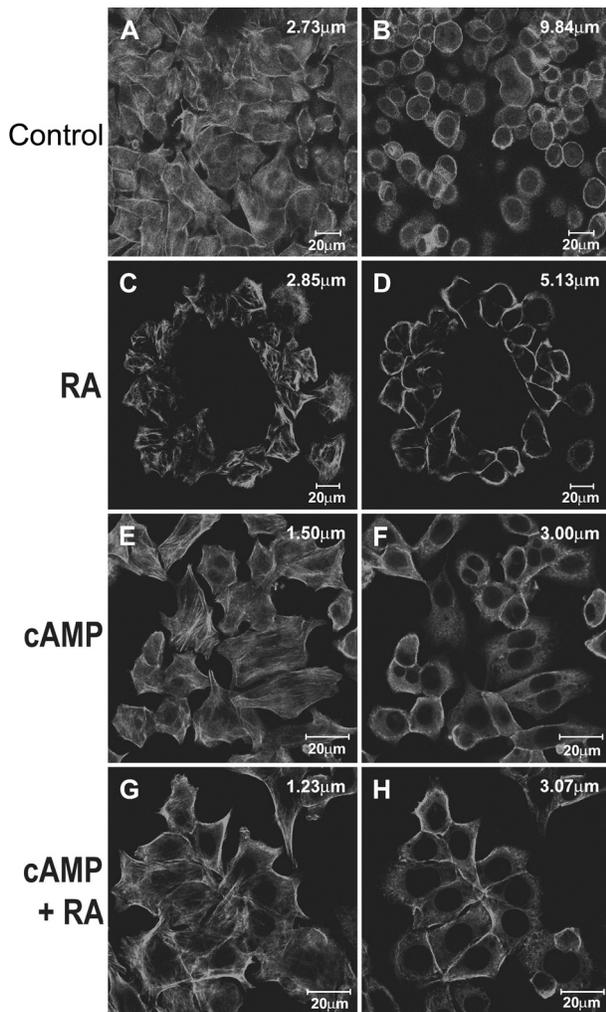


**Figure 3.** Laser scanning confocal microscopy images of HTC cells showing the pattern of actin filament distribution at T48. Left and right panels represent different optical sections on the Z-axis obtained during image capture: control cells (*A* and *B*), retinoic acid (*C* and *D*), cAMP (*E* and *F*), and retinoic acid plus cAMP (*G* and *H*). In the control culture shown in *B*, it is possible to observe the presence of rounded cells growing partially adhered to the substrate, which were not observed in treated cultures (*C-H*). The treatments induced actin reorganization (actin stress fiber formation) and changes in cell shape (*C*, *E* and *G*). Note the presence of binucleated cells in cultures treated with cAMP (*F*).
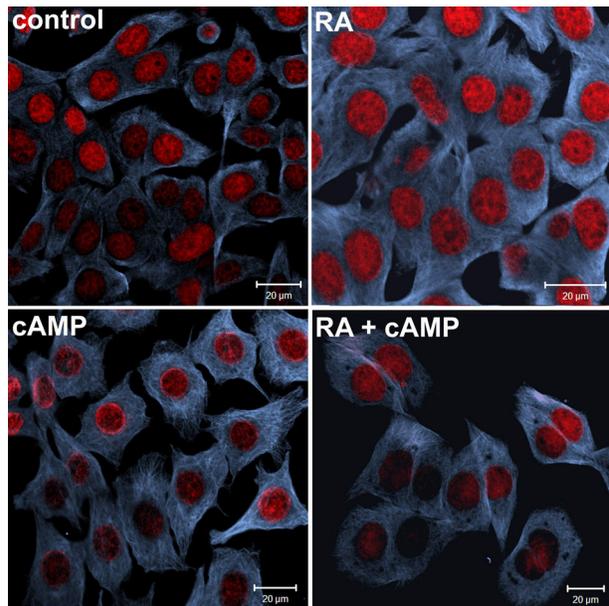


**Figure 4.** Images of HTC cells showing microtubule distribution at T48. The microtubule network is more evident in treated cells than in control cells, suggesting that retinoic acid (RA) and cAMP induced microtubule reorganization.
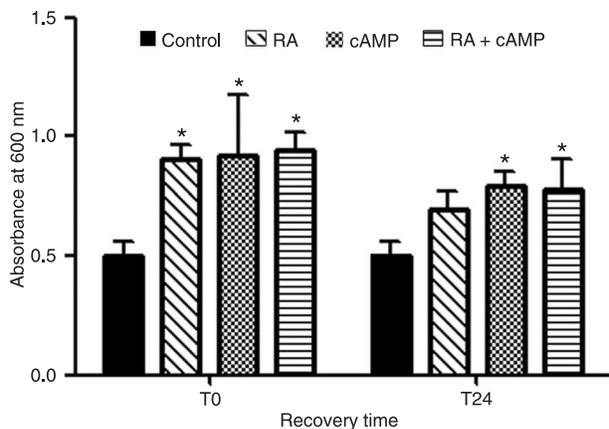


**Figure 5.** The adhesion assay using a laminin substrate showed increased cell-to-substrate interaction of treated cells. *P < 0.05 compared to control (Bonferroni test).

in cultures treated with cAMP and RA plus cAMP. Also, Cx26 was expressed in all treated cells and its expression was highest in cells treated with cAMP at T24 (Figure 6). At T48, Cx32 expression was up-regulated in cells treated



**Figure 6.** Immunoblot showing the expression pattern of connexins (Cx), E-cadherin and vinculin in treated and control cells. α-tubulin was used as the control for sample application.

with cAMP, RA and RA plus cAMP. At the same time, Cx43 expression was down-regulated in all groups of treated cells (Figure 6). The treatments did not change the pattern of vinculin expression; however, at T24 we detected slightly increased E-cadherin expression in treated cultures, mainly in RA- and cAMP-treated cells. At T48, E-cadherin was preferentially expressed in cAMP-treated cells (Figure 6). Table 1 summarizes the modifications found in expression profiles in HTC cells treated with RA and cAMP.
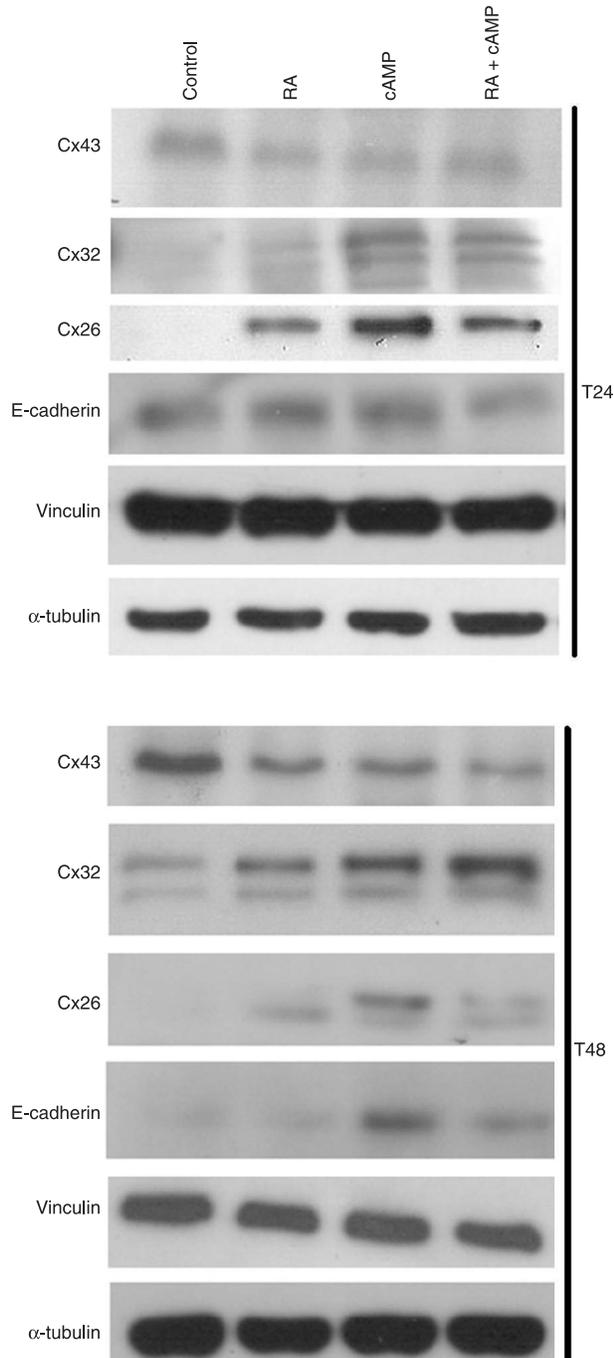
**Telomerase activity**

Telomerase activity was another parameter associated with both cell proliferation capacity and cell differentiation status. The results obtained showed that both cAMP and RA can inhibit telomerase activity. cAMP presented strong inhibition capacity at T0 while RA was effective in regulating telomerase activity negatively at T48. Interestingly, telomerase activity was inhibited in cells treated with RA plus cAMP from T0 to T48. Figure 7 shows relative telomerase activity at the various recovery times.

**Expression of signaling proteins (ERK and GSK-3β)**

We investigated the expression profiles of total ERK, pERK and GSK-3β phosphorylated at Ser9 or Tyr216. All treated cells showed lower phosho-ERK expression levels compared to control cells. However, cells treated with cAMP showed decreased pERK expression compared with samples treated with RA and RA plus cAMP (Figure 8). We investigated the expression of both forms of GSK-3β (active and inactive), which corresponds to GSK-3β phosphorylated at Tyr216 and Ser9 residues, respectively. Ser9-GSK-3β expression levels were lower in control cells than treated cells. The cells treated with RA plus cAMP had the highest Ser9-GSK-3β expression levels (Figure 8). There were only slight changes in Tyr216-GSK-3β expression levels between control cells and cells treated with RA plus cAMP (Figure 8). Changes in the expression profiles of pERK and pGSK induced by the treatments are summarized in Table 1.

## Discussion

In the present study, we investigated the effects of RA and/or cAMP on the proliferative behavior and phenotype of HTC cells. We also evaluated a possible synergistic effect between RA and cAMP. The treatment schedule was designed according to results obtained from BRL3A that showed high responsiveness to co-treatment. Therefore, HTC cells were treated for 48 h with RA or cAMP (in combination or not) followed by 24- and 48-h recovery in fresh medium.

HTC cells treated with RA and cAMP exhibited changes both in cell morphology and in gene expression profiles that were consistent with a differentiated phenotype. It is important to note that these events were preferentially observed at the recovery times (T24 and T48), indicating that

the effects of RA and cAMP on the proliferative behavior and phenotype of HTC cells continued after the treatment period. This aspect is very important to establish preclinical and clinical protocols that include RA and/or cAMP as chemotherapeutic agents.

During the recovery period we observed a decrease in Cx43 expression with a concomitant induction of Cx32 and Cx26 expression. This change in connexin expression profile occurred independently of the combined use of RA and cAMP; however, the highest Cx32 expression levels were observed at T48 in cultures treated with RA plus cAMP. In the liver, Cx43 is expressed by oval cells (hepatic stem-cells), endothelial cells and biliary cells, but not by hepatocytes. Cx32 and Cx26 are major connexin isoforms expressed by hepatocytes. Cx32 is expressed by hepatocytes of the hepatic acini while Cx26 is expressed by hepatocytes of the periportal spaces (17). Our results are very important because there are almost no data in the literature that demonstrate the modulation of connexin expression profile as a consequence of RA and/or cAMP treatment in hepatic tumor cells. We demonstrated that a mixture consisting of RA and cAMP was very effective in inducing Cx32 expression. Ara et al. (18) observed an increase of the Cx32 phosphorylated isoform in HepG2 cells after treatment with RA and they considered this event to be an important aspect of the reversal of the transformed phenotype of HepG2 cells.

In another independent study, Lee et al. (11) observed that HepG2 cells treated with cAMP for 3 days presented growth arrest as a consequence of both cyclin-dependent kinase (cdk) inhibitor up-regulation (p27Kip1, P21 Waf1/Cip1) and cyclin A down-regulation, although they did not report morphological changes associated with a differentiated phenotype.

HepG2 was also used as a model by Alisi et al. (19), who detected growth inhibition of HepG2 cells after 7 days of treatment with RA. They demonstrated that RA influenced the activities of cyclin-cdk complexes involved in the regulation of G1/S transition and S-phase progression, mainly by modifying the binding of these complexes to p21 and p27 inhibitors. Thus, morphological analysis was not performed by Lee et al. (11) or by Alisi et al. (19), who worked independently to determine the effects of RA or cAMP on hepatic tumor cells. The present study shows for the first time the results obtained with the separate or concomitant use of RA and cAMP on the proliferative behavior and phenotype of hepatocarcinoma cells.

Telomerase activity is a hallmark of the immortal phenotype and its suppression has been considered an important parameter to detect the efficacy of RA in inducing cell differentiation and reversal of transformed phenotype in leukemia cells as well as in breast cancer and neuroblastoma cells (20-22). We determined that cAMP exerts a strong negative effect on telomerase activity, which was observed at T0. RA also inhibited telomerase activity; however, this effect

**Table 1.** Modifications of the expression profiles of HTC cells treated with retinoic acid (RA) and cAMP.

| | RA | cAMP | RA + cAMP |
|---|---|---|---|
| Cx43 | ↓ | ↓ | ↓ |
| Cx32 | ↑ | ↑ | ↑ |
| Cx26 | ↑ | ↑ | ↑ |
| E-cadherin | Slightly ↑ | ↑ | ↑ |
| Vinculin | No alteration | No alteration | No alteration |
| pERK | ↓ | ↓ | ↓ |
| Ser9-GSK-3β | ↑ | ↑ | ↑ |
| Tyr216-GSK-3β | Slightly ↓ | Slightly ↓ | Slightly ↓ |

The quantitative analysis was performed using ImageJ, a public domain program. Cx = connexin; pERK = phosphorylated extracellular signal-regulated kinase; GSK-3β = glycogen synthase kinase 3 beta.
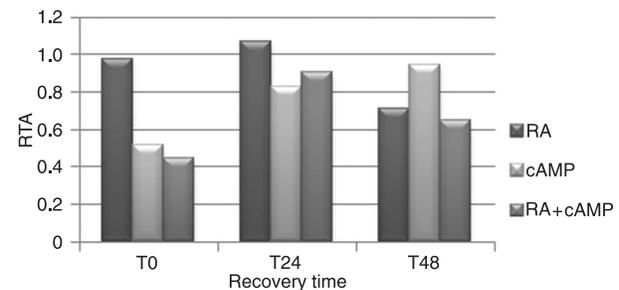


**Figure 7.** Relative telomerase activity (RTA) was determined using the TeloTAGGG Telomerase PCR ELISA[PLUS] kit and was calculated according to the following formula: RTA = [(Abs sample - Abs RNAase-treated sample) / Abs internal standard of the sample] / [(Abs control template - Abs lysis buffer) / Abs internal standard of the control template] x 100, where Abs = absorbance. RA = retinoic acid.
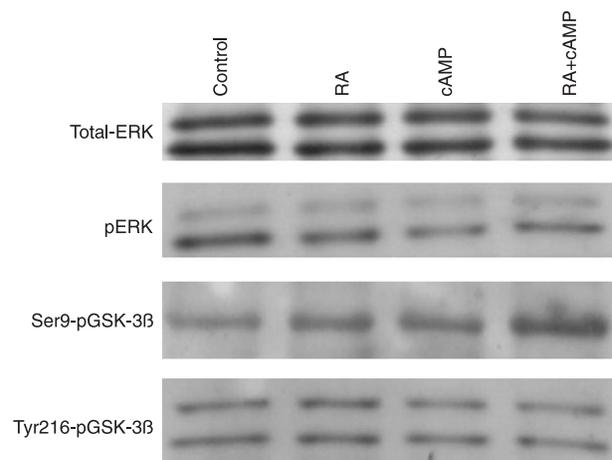


**Figure 8.** Immunoblot showing the expression patterns of signaling extracellular signal-regulated kinase (ERK) and glycogen synthase kinase 3 beta (GSK-3β) protein at T24. pERK = phosphorylated ERK; RA = retinoic acid. Total- ERK was the sample loading control.

was only seen at T48. Thus, cells treated with the mixture (RA plus cAMP) presented inhibition of telomerase activity from T0 to T48. The concomitant use of RA and cAMP can be useful to improve the effect of treatment, mainly with low RA concentrations. In this study, for example, RA was used at 0.1 µM.

Treatment with RA and/or cAMP promoted microfilament reorganization in HTC cells. This event seems to be critical to cell shape modification because the treated cells became flattened, exhibited polyhedric morphology and presented higher adhesion capacity, both cell-to-cell and cell-to-substratum. It is possible that the protein complexes involved in intercellular contacts and cell polarity were stabilized by cytoskeleton reorganization. We saw important up-regulation of E-cadherin expression in cultures treated with cAMP, even though we did not observe changes in vinculin expression in these cultures. Similar data were obtained by Masuda et al. (23), who observed E-cadherin up-regulation in hepatocellular carcinoma cells (HCC-T and HCC-M) treated with sodium butyrate.

Assays for cell adhesion to a laminin substrate confirmed the effect of treatment. After treatment with RA and/or cAMP, the cells presented higher adhesion capacity than untreated cells. Good adhesive ability may be a relevant and appropriate characteristic of well-differentiated cells. Our data agree with Massimi and Divirgiliis (24), who demonstrated increased adhesiveness of HepG2 cells after treatment with RA for 12 days. A similar experimental approach has not been previously used with cAMP. Considering that the RAF/MEK/ERK pathway is constitutively activated in HCC (25-27), we investigated whether the drugs used in this study had some effect on ERK phosphorylation. We observed lower pERK expression levels in treated cells compared to control cells. This result suggests that the antiproliferative effects of RA and cAMP on HTC cells may be due, at least in part, to their capacity to negatively regulate ERK phosphorylation. Similar results were observed by Kanamori et al. (28), who showed cell proliferation inhibition by acriflavine, a synthetic retinoid, with concomitant ERK phosphorylation inhibition in human HCC cells (HuH7).

In the present study, treatment with cAMP was more effective in inhibiting ERK phosphorylation than RA treatment or co-treatment. Thus, we extended our study and also investigated the effect of these drugs on GSK-3β, whose activity is modulated by several signaling pathways including the Wnt, PI-3K/AKT and Ras/MAPK pathways (29). GSK-3β activity is regulated by site-specific phosphorylation of Tyr216/Ser9 residues (30). The active and inactive forms are characterized by a phosphorylation pattern at the Tyr216 and Ser9 residues, respectively. GSK-3β drives oncogenic progression either by its inhibition or its activation, depending on the tumor (31). In gastrointestinal cancers (pancreatic, colorectal and hepatic), lower pSer9-GSK-3β expression is commonly observed compared to the active form (32). In fact, we observed low pSer9-GSK-3β expression in control cells while in treated cells pSer9-GSK-3β expression levels were up-regulated. Interestingly, cells treated with RA plus cAMP exhibited higher pSer9-GSK-3β expression than cells treated with only RA or cAMP.

The interaction of drugs with the cellular environment is extremely complex and requires extensive investigation. The exploration of the recovery times permitted us to evaluate in more detail a possible interaction between RA and cAMP. For example, if we evaluated independently each time we could conclude that there is no synergistic effect between RA and cAMP. However, when we analyzed the kinetics of the events along the recovery time we noted that co-treatment contributed to extending the period during which cell growth was inhibited and increased the degree of HTC cell differentiation.

The present study demonstrated that RA and cAMP can inhibit cell proliferation and are also effective in inducing differentiation of HTC cells. However, when they are used in combination the signals regarding cell proliferation inhibition are temporally amplified and the degree of cell differentiation is increased.

## Acknowledgments

## References

1. Ferlay J, Shin HR, Bray F, Forman D, Mathers C, Parkin DM. Estimates of worldwide burden of cancer in 2008: GLOBOCAN 2008. *Int J Cancer* 2010; 127: 2893-2917.

2. Wong CM, Ng IO. Molecular pathogenesis of hepatocellular carcinoma. *Liver Int* 2008; 28: 160-174.

3. Noy N. Between death and survival: retinoic acid in regulation of apoptosis. *Annu Rev Nutr* 2010; 30: 201-217.

4. Bushue N, Wan YJ. Retinoid pathway and cancer therapeutics. *Adv Drug Deliv Rev* 2010; 62: 1285-1298.

5. Wang ZY, Chen Z. Acute promyelocytic leukemia: from highly fatal to highly curable. *Blood* 2008; 111: 2505-2515.

6. Wang A, Zeng R, Huang H. Retinoic acid and sodium butyrate as cell cycle regulators in the treatment of oral squamous carcinoma cells. *Oncol Res* 2008; 17: 175-182.

7. Ventura-Holman T, Mamoon A, Subauste JS. Modulation of expression of RA-regulated genes by the oncoprotein v-erbA. *Gene* 2008; 425: 23-27.

8. Lu J, Zhang F, Zhao D, Hong L, Min J, Zhang L, et al. ATRA-inhibited proliferation in glioma cells is associated with subcellular redistribution of beta-catenin via up-regulation of Axin. *J Neurooncol* 2008; 87: 271-277.

9. Jung HY, Park SH, Yoo YD, Kim JS, Kim YH. CDK2/4

regulate retinoic acid-induced G1 arrest in hepatocellular carcinoma cells. *Hepatol Res* 2005; 31: 143-152.

10. Quenech'Du N, Ruchaud S, Khelef N, Guiso N, Lanotte M. A sustained increase in the endogenous level of cAMP reduces the retinoid concentration required for APL cell maturation to near physiological levels. *Leukemia* 1998; 12: 1829-1833.

11. Lee J, Choi YH, Nguyen P, Kim JS, Lee SJ, Trepel JB. Cyclic AMP induces inhibition of cyclin A expression and growth arrest in human hepatoma cells. *Biochim Biophys Acta* 1999; 1449: 261-268.

12. Liu L, Xie Y, Lou L. Cyclic AMP inhibition of proliferation of hepatocellular carcinoma cells is mediated by Akt. *Cancer Biol Ther* 2005; 4: 1240-1247.

13. Kovach SJ, Price JA, Shaw CM, Theodorakis NG, McKillop IH. Role of cyclic-AMP responsive element binding (CREB) proteins in cell proliferation in a rat model of hepatocellular carcinoma. *J Cell Physiol* 2006; 206: 411-419.

14. Thompson EB, Tomkins GM, Curran JF. Induction of tyrosine α-ketoglutarate transaminase by steroid hormones in a newly established tissue culture cell line. *Biochemistry* 1966; 56: 296-303.

15. Prado MP, Torres YR, Berlinck RGS, Desidera C, Sanchez MA, Craveiro MV, et al. Effects of marine organisms extracts on microtubule integrity and cell cycle progression in cultured cells. *J Exp Mar Biol Ecol* 2004; 313: 125-137.

16. Machado-Santelli GM, Mori L, Pereira CA. Prediction of relapse in patients with breast cancer by DNA cytometry. *Anal Cell Pathol* 1994; 7: 321-334.

17. Neveu MJ, Sattler CA, Sattler GL, Hully JR, Hertzberg EL, Paul DL, et al. Differences in the expression of connexin genes in rat hepatomas *in vivo* and *in vitro*. *Mol Carcinog* 1994; 11: 145-154.

18. Ara C, Massimi M, Devirgiliis CL. Retinoic acid modulates gap junctional intercellular communication in hepatocytes and hepatoma cells. *Cell Mol Life Sci* 2002; 59: 1758-1765.

19. Alisi A, Leoni S, Piacentani A, Conti DL. Retinoic acid modulates the cell-cycle in fetal rat hepatocytes and HepG2 cells by regulating cyclin-cdk activities. *Liver Int* 2003; 23: 179-186.

20. Yamada O, Ozaki K, Nakatake M, Akiyama M, Kawauchi K, Matsuoka R. Multistep regulation of telomerase during differentiation of HL60 cells. *J Leukoc Biol* 2008; 83: 1240-1248.

21. Phipps SM, Love WK, White T, Andrews LG, Tollefsbol TO. Retinoid-induced histone deacetylation inhibits telomerase activity in estrogen receptor-negative breast cancer cells. *Anticancer Res* 2009; 29: 4959-4964.

22. Das A, Banik NL, Ray SK. Retinoids induce differentiation and downregulate telomerase activity and N-Myc to increase sensitivity to flavonoids for apoptosis in human malignant neuroblastoma SH-SY5Y cells. *Int J Oncol* 2009; 34: 757-765.

23. Masuda T, Saito H, Kaneko F, Atsukawa K, Morita M, Inagaki H, et al. Up-regulation of E-cadherin and I-catenin in human hepatocellular carcinoma cell lines by sodium butyrate and interferon-alpha. *In Vitro Cell Dev Biol Anim* 2000; 36: 387-394.

24. Massimi M, Devirgiliis LC. Adhesion to the extracellular matrix is positively regulated by retinoic acid in HepG2 cells. *Liver Int* 2007; 27: 128-136.

25. McKillop IH, Schmidt CM, Cahill PA, Sitzmann JV. Altered expression of mitogen-activated protein kinases in a rat model of experimental hepatocellular carcinoma. *Hepatology* 1997; 26: 1484-1491.

26. Ito Y, Sasaki Y, Horimoto M, Wada S, Tanaka Y, Kasahara A, et al. Activation of mitogen-activated protein kinases/extracellular signal-regulated kinases in human hepatocellular carcinoma. *Hepatology* 1998; 27: 951-958.

27. Feng DY, Zheng H, Tan Y, Cheng RX. Effect of phosphorylation of MAPK and Stat3 and expression of c-fos and c-jun proteins on hepatocarcinogenesis and their clinical significance. *World J Gastroenterol* 2001; 7: 33-36.

28. Kanamori T, Shimizu M, Okuno M, Matsushima-Nishiwaki R, Tsurumi H, Kojima S, et al. Synergistic growth inhibition by acyclic retinoid and vitamin K2 in human hepatocellular carcinoma cells. *Cancer Sci* 2007; 98: 431-437.

29. Cohen P, Frame S. The renaissance of GSK3. *Nat Rev Mol Cell Biol* 2001; 2: 769-776.

30. Doble BW, Woodgett JR. GSK-3: tricks of the trade for a multi-tasking kinase. *J Cell Sci* 2003; 116: 1175-1186.

31. Kang T, Wei Y, Honaker Y, Yamaguchi H, Appella E, Hung MC, et al. GSK-3 beta targets Cdc25A for ubiquitin-mediated proteolysis, and GSK-3 beta inactivation correlates with Cdc25A overproduction in human cancers. *Cancer Cell* 2008; 13: 36-47.

32. Mai W, Kawakami K, Shakoori A, Kyo S, Miyashita K, Yokoi K, et al. Deregulated GSK3{beta} sustains gastrointestinal cancer cells survival by modulating human telomerase reverse transcriptase and telomerase. *Clin Cancer Res* 2009; 15: 6810-6819.